

RESEARCH PAPER

Spectrophotometric Determination of Silver (I) With 2-Hydroxy-5-(5-(4-Methoxy-3-Nitrophenyl)-1,3,4-Thiadiazol-2-yl) Diazenyl Benzoic Acid (HMNTDABA) as a Nano Organic Reagent

Mina Kadhim Hadi *, Shaimaa Mohsen Essa

Department of Chemistry, College of Education, University of Al-Qadisiyah, Diwaniyah, Iraq

ARTICLE INFO

Article History:

Received 12 February 2025

Accepted 09 June 2025

Published 01 July 2025

Keywords:

Characterization

Silver (I)

Spectrophotometric

determination

Thiadiazol

ABSTRACT

This study proposed the use of a sensitive and selective spectroscopic method for the determination of silver (I) using the novel nano azo reagent 2-hydroxy-5-(5-(4-methoxy-3-nitrophenyl)-1,3,4-thiadiazol-2-yl) diazenyl benzoic acid (HMNTDABA) as a spectroscopic nano reagent. The nano reagent was synthesized and characterized by using UV-Vis. spectroscopy, fourier transform infrared spectroscopy (FTIR), ¹H-NMR spectroscopy, X-ray diffraction (XRD) and field emission scanning electron microscopy (FESEM) and Elemental Analysis (CHNS). The reaction between the synthesized nano reagent and the silver (I) takes place instantaneously when λ_{max} is 563 nm and solution pH is 8. The prepared nano reagent results in the formation of the complex with D.L = 0.085ppm, S.D and R.S.D. of 0.001 and 0.14% respectively. The obtained recovery range (%R) was 99.965%. The stability constant of the prepared 1:1 [metal: reagent] of Ag(I) complex was $0.5 \times 10^{-6} \text{ L mol}^{-1}$. The linear range was found to be between 1 and 80 ppm. The primary interferences were primarily due to the presence of Fe²⁺, Ni²⁺, Zn²⁺, Pb²⁺, Cu²⁺, and Cd²⁺ ions. To address these interferences, appropriate masking agents were employed.

How to cite this article

Hadi M., Essa S. Spectrophotometric Determination of Silver (I) With 2-Hydroxy-5-(5-(4-Methoxy-3-Nitrophenyl)-1,3,4-Thiadiazol-2-yl) Diazenyl Benzoic Acid (HMNTDABA) as a Nano Organic Reagent. J Nanostruct, 2025; 15(3):916-927. DOI: 10.22052/JNS.2025.03.010

INTRODUCTION

Organic reagents are chemical compounds that have been used for both quantitative and qualitative analysis of elements resulting in the formation of the colored complex [1-4]. Due to this reason, these reagents are widely employed for determining even the minute concentrations of several metal ions in different kinds of the materials [1, 5, 6]. The azo compounds-based complexes were reported to play a vital role in the biological fields because they have atoms like oxygen, nitrogen and sulfur, that allow them to bind with various metal ions [7, 8]. When

* Corresponding Author Email: minakadhimhadi@gmail.com

comes to the selection of the metal, silver (Ag) is little harder than gold (Au). It is very ductile and malleable when compared with Au and palladium (Pd). Additionally, the electrical and thermal conductivity of the Ag metal is superior to all other metals while having the smallest contact resistance [9-11]. Ag is mainly sourced out from the copper ores [12] and finds wide range of applications in dental compounds, mirrors, electrical contacts, batteries, photography, jewelry, printed circuit, electronic industries [13-16] and for preventing bacterial development or growth in a variety of commercial products, like textiles [17]. Ag, at



This work is licensed under the Creative Commons Attribution 4.0 International License.

To view a copy of this license, visit <http://creativecommons.org/licenses/by/4.0/>.

higher concentration, usually upto 2g of soluble Ag salts (in form of AgNO_3), proved to be deadly. Ag compounds get easily absorb in the body tissues resulting in the bluish or blackish skin pigmentation [18-20]. Various methods including high performance liquid chromatography (HPLC) [21], kinetic [22-25], flame atomic absorption [26], solid phase extraction (SPE) [27], fluorimetric [28], electric method [29] and the spectrophotometric method [30-35] have been developed nowadays that determine the presence of the Ag ion. Among these methods, the spectrophotometric method was used in this study. Keeping in view the above discussion, the present study aimed to (i) synthesize new organic reagent (HMNTDABA), (ii) characterize the newly synthesized reagent by different techniques including FT-IR, UV-Vis, $^1\text{H-NMR}$ spectra, XRD and FESEM techniques for determining the extent of this reagent's interaction

with 16 elements of the periodic table (iii) explore the interaction of this reagent with the Ag ion and (iv) determine the levels of Ag in some materials including dental filling.

MATERIALS AND METHODS

Instruments

Functional group study of the synthesized nano reagent was carried out by using Shimadzu Fourier transform infrared spectrophotometer (FTIR-8400S, Japan) within the spectral range of $400\text{-}4000\text{ cm}^{-1}$ in KBr disks [36-40]. The UV-Vis absorption spectra were measured by using Shimadzu UV-1800 UV/Visible scanning spectrophotometer while the absorbance was measured using 1 cm quartz cells. Further, MIRA3 device was used for the Field emission scanning electron microscopy (FESEM) analysis of the prepared materials. The CHNS analyzer,

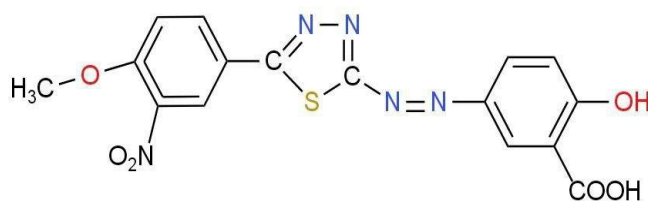


Fig. 1. Structure of the nano organic reagent HMNTDABA

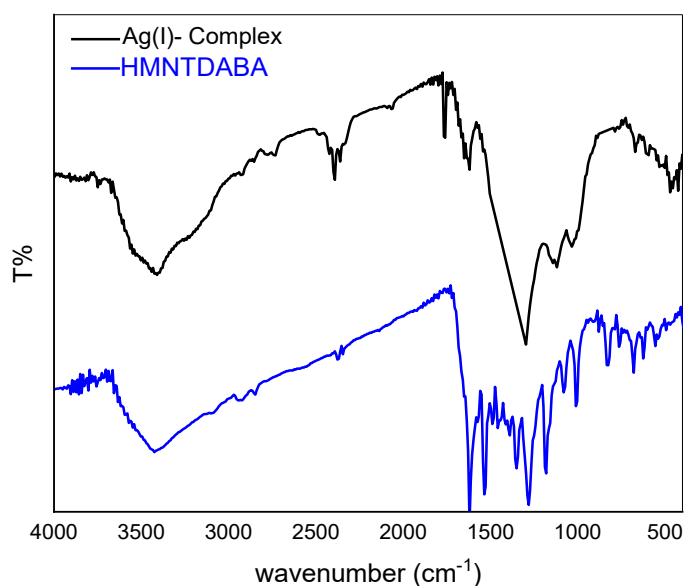


Fig. 2. FTIR spectra of the newly synthesized reagent, HMNTDABA and its Ag (I) complex.

BBOT Model, was used to determine the carbon, hydrogen, nitrogen, and sulfur content in chemical samples. The X-ray diffraction (XRD) pattern of the prepared materials, a device (D2 Phaser) at an angular range of $2\theta = 10-80^\circ$ was used. The pH of each solution was measured by using the pH meter (pH-3110 WTW, Germany) while the melting point measurements were carried out by using SMP30 Stuart, UK.

Reagents and solution preparation

All the chemicals used in the study were of analytical grade, and used without any further purification. Ethanol was purchased from Germany. The standard solution of organic reagent (HMNTDABA) having concentration of 1×10^{-4} M was prepared by dissolving 0.040g in 250 mL of absolute ethanol. For the preparation of the stock solution of Ag(I) having concentration of $1000 \mu\text{g mL}^{-1}$, nearly 0.157g of AgNO_3 (Merck) was dissolved in 100 mL of deionized water. Other Ag (I) solutions were prepared by diluting the stock solution with distilled water. The pH of the solutions (3.4-10.5) was adjusted with ammonium acetate (0.01 mol L^{-1}) ammonia-glacial acetic acid buffer solution.

General procedure

Firstly, the volumetric bottle with capacity of 10mL was taken to which 2mL of silver ion (I) solution having concentration of 100 ppm was added. This was followed by the addition of 3mL HMNTDABA nano reagent (Fig. 1) solution with a concentration of 1×10^{-4} M. The total volume of the solution was made up to the mark with distilled water. The final concentration of the obtained complex was 100 ppm having pH solution of 8. The absorbance of the resulting solution was then measured after 5 min at the λ_{max} of 563nm at the temperature of 25°C against the nano reagent solution prepared in the same way in the reference cell (without silver solution).

RESULTS AND DISCUSSION

FTIR and FESEM analysis of the newly synthesized nano reagent (HMNTDABA) and its complex

The functional group study of the synthesized nano reagent and its complex was carried out within the range $400-4000 \text{ cm}^{-1}$ [41-44]. The results of the FTIR study for the synthesized reagent and its complex are elaborated in Fig. 2. The bands of the azo reagent at 3425.3 cm^{-1} and 3240.2 cm^{-1} corresponds to the presence of the

O-H bond of the carboxylic acid and the alcoholic O-H bond, respectively. The peaks obtained within the range 3016.46 cm^{-1} to 3062.75 cm^{-1} corresponds to the aromatic C-H bond vibrations while the peaks ranging from 1442.66 cm^{-1} to 1550 cm^{-1} corresponds to the N=O and N=N bond vibrations of the nitro group and the azo group respectively. Furthermore, the peaks within the range 1660 cm^{-1} to 1658.67 cm^{-1} corresponds to the presence of the C=C and C=O vibrations. The functional group study of the silver complex revealed the change/ shift in the apparent peaks of the nano reagent. The peaks obtained within the range 3200 cm^{-1} to 3550 cm^{-1} revealed the presence of the O-H group in the complex while the bonds appeared within the range 470 cm^{-1} to 672 cm^{-1} showed the presence of the Ag-N and Ag-O bond vibrations respectively. The FESEM images of the nano reagent in Fig. 3 reveal the morphological characteristics of the studied compound and its microstructural characteristics. The surface of the nano reagent is heterogeneous possessing numerous irregularities. Particle sizes, however, appears to be consistent across the sample highlighting the controlled synthesis process. Additionally, the presence of the clusters in images also highlights the aggregation behavior of the particles that would affect the properties of the materials. The FESEM images of the prepared complex reveal the agglomeration of Ag particles on the surface of the nano reagent. This observation supports the coordination between the nano reagent and the Ag particles Fig. 3 [45-48].

Elemental analysis

Elemental analysis of a compound helps in determining the type of elements and their respective percentages in compound. The results of the elemental analysis (as summarized in Table 1) show that the studied compound is chiefly composed of carbon (C), hydrogen (H), nitrogen (N) and sulfur (S) in percentages of 46.999%, 2.723%, 17.139% and 7.677% respectively. Furthermore, the calculated molecular weight of compound i.e., 401.364 g/mol is consistent with the molecular formula i.e., $\text{C}_{16}\text{H}_{11}\text{SN}_5\text{O}_6$.

$^1\text{H-NMR}$ spectrum and XRD analysis for organic reagent

The synthesized nano reagent i.e., HMNTDABA in DMSO-d6 solvent was analyzed by using

¹H-NMR spectrum and the results are shown in Fig. 4. The results elaborated in the Fig. 4 show the signal appear at a location of 52 ppm. The ¹H-NMR spectrum of HMNTDABA showed the band at a frequency of 98 ppm representing the presence of the OCH3 group. Additionally, the bands appeared at 97ppm and 45ppm represents the proton number 15. The location of 1.4 ppm belongs to the OH proton while the presence of the proton of the thiazole ring take place at a frequency of

57.8 ppm. The XRD analysis of the prepared nano reagent, HMNTDABA, has been outlined in Fig. 5. The results of the study highlight the complex crystalline structure of the HMNTDABA having numerous diffraction peaks at various 2θ positions, notably at 11.5744°, 31.8404°, and 38.3375°, with the highest intensity observed at 38.3375°. The results of the XRD provide important information regarding the crystallinity and structural properties of the newly synthesized nano reagent [49-51].

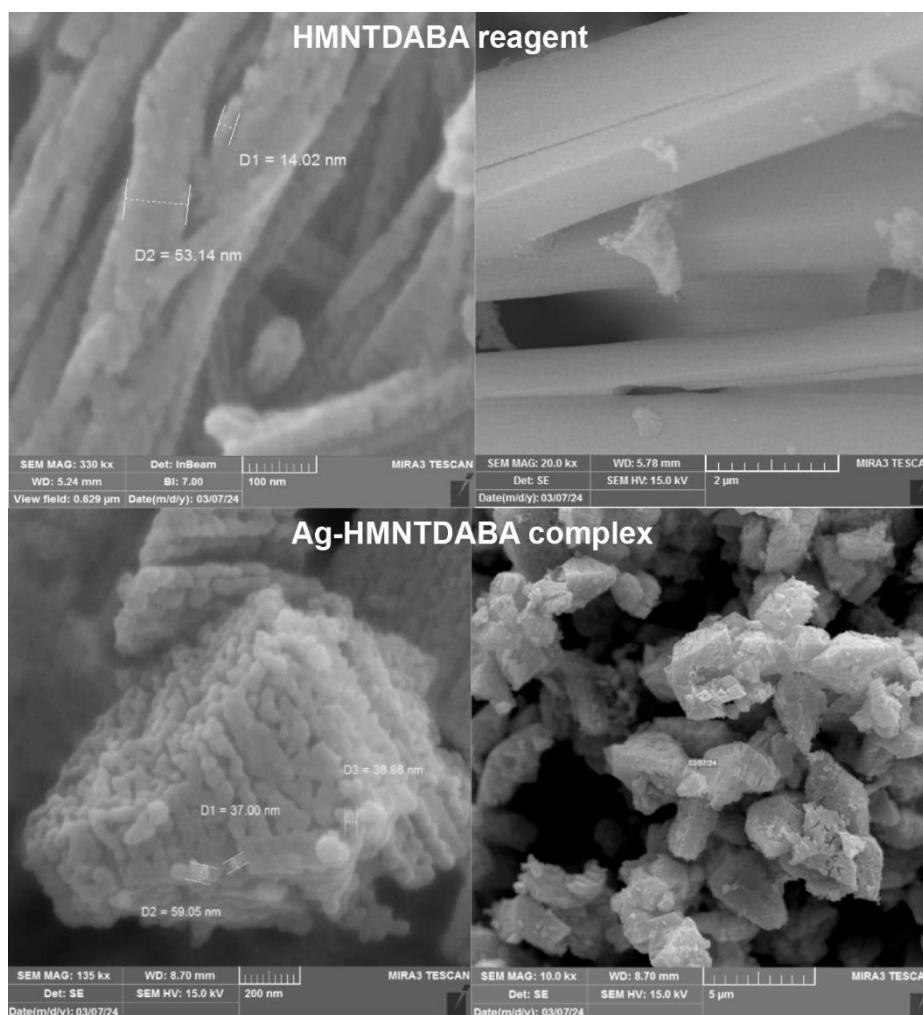


Fig. 3. FESEM images of the newly synthesized nano reagent, HMNTDABA and its Ag (I) complex.

Table 1. C H N S analysis of the compound.

Compound	M. wt	C%		H%		N%		S%	
		Found	Calc	Found	Calc	Found	Calc	Found	Calc
C ₁₆ H ₁₁ SN ₅ O ₆	401.364	46.999	47.880	2.723	2.765	17.139	17.449	7.677	7.987

Absorption spectra and characteristics of the nano reagent and relative complex

Fig. 6 revealed the absorption spectrum of the silver complex (I) with the nano reagent, obtained within the wavelength range of 200-800 nm. Results of the study revealed the presence of the red shift in the spectrum due to the electronic transition i.e., $\pi \rightarrow \pi^*$ at the λ_{max} of 563 nm. As compared to the Planck solution as a reference, the solution with pH=8 was at the highest absorption peak. Furthermore, when the absorption spectrum of the nano reagent was compared with the absorption spectrum of the

complex, a clear difference in the values of λ_{max} for both the nano reagent and the complex was observed. Additionally, the red shift occurred towards the longer wavelength in the spectra. These results are the evidence of the occurrence of a coordination process taking place between the metal ion and the nano reagent during the synthesis of the complex[38].

Parameters

Effect of pH

The results of the pH study in Fig. 7 reveal the effect of acid function values on the absorbency

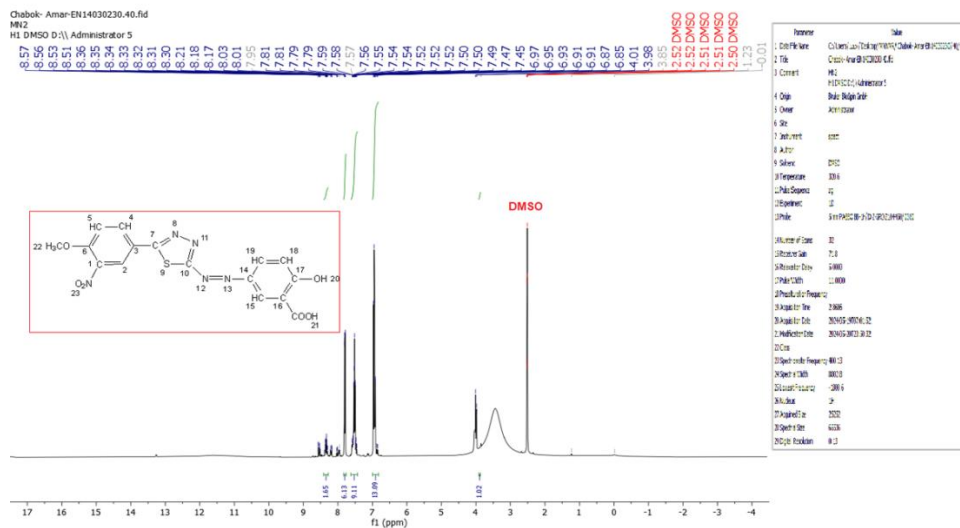


Fig. 4. ¹H-NMR spectrum of nano organic reagent HMNTDABA.

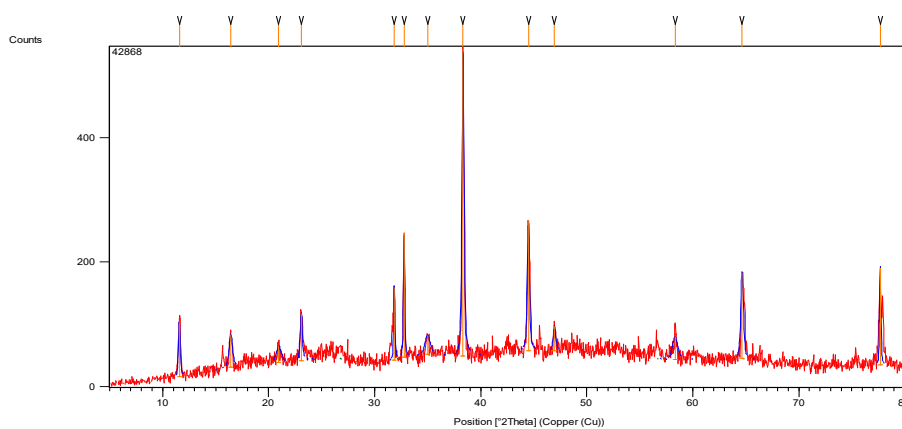


Fig. 5. XRD pattern of nano organic reagent HMNTDABA

of the silver (I) complex. It was observed that the color intensity of the complex solution increases gradually reaching its peak at the acid level of 8 afterwards a decrease in the absorbance value of the complex take place. This decrease might be due to the deposition of the element ion or due to the formation of unstable complex ions [49].

Effect of the temperature and time

The effect of the temperature on the absorption of a silver complex solution has been shown in Fig. 8. Results of the study revealed that the absorption values of the silver complex solution give the best color intensity at temperature range of 10-40 °C afterwards it starts decreasing with further

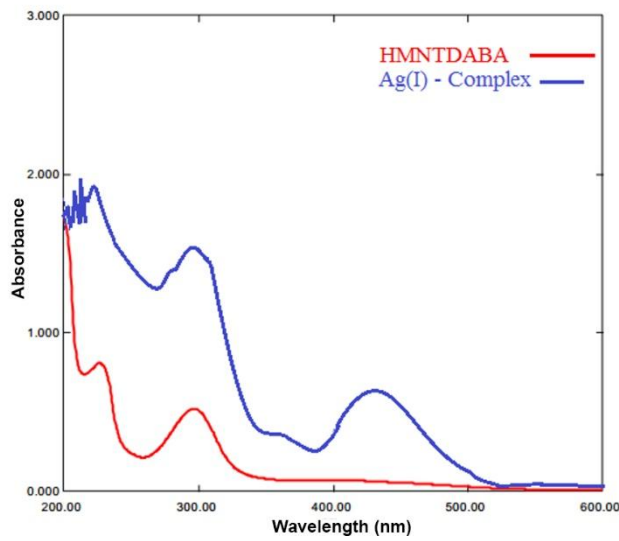


Fig. 6. Absorption spectra of Ag(I) ion having concentration of 20 ppm with the nano reagent at pH=8

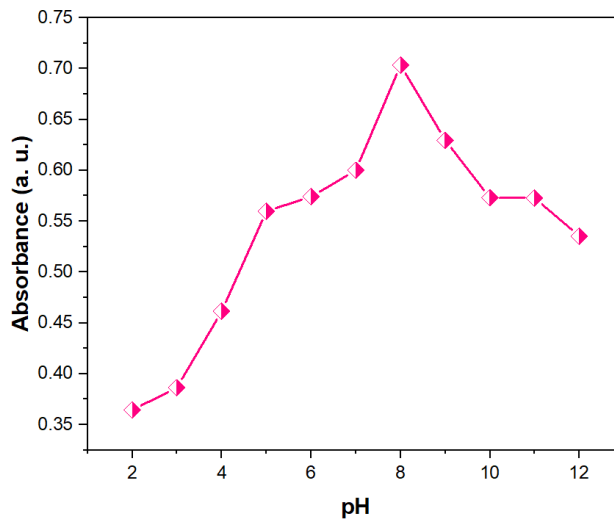


Fig. 7. Effect of pH on the absorption of the Ag complex solution (Ag concentration of 20 ppm + 3 mL of nano reagent solution with concentration of 1×10^{-4} M).

increase in temperature. This effect can be better explained by the disintegration of the complex at the high temperatures or the conversion of some part of the complex into another form when the

solution temperatures exceeds 40 °C [52].

The effect of the time on the stability of the absorbance of the silver complex (I) solution is shown in Fig. 9. Results of the study revealed

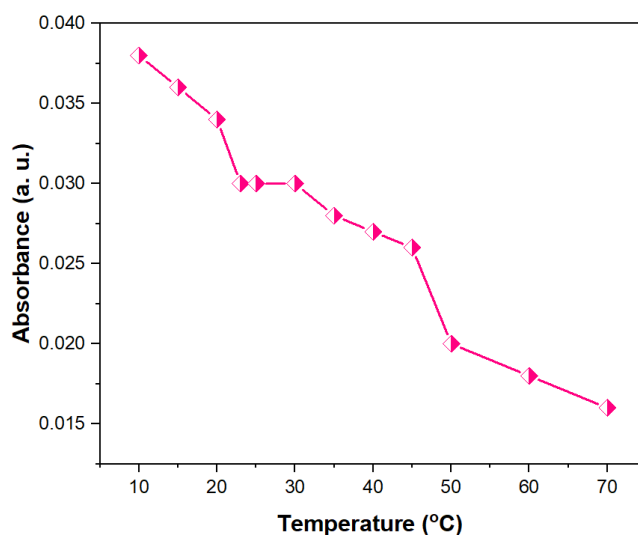


Fig. 8. Effect of temperature on the absorption of the Ag complex solution (Ag concentration of 20 ppm + 2 mL nano reagent solution with concentration of 1×10^{-4} M).

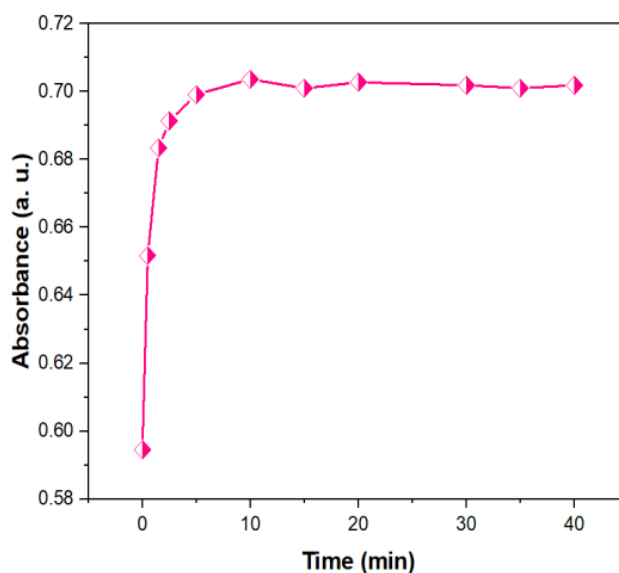


Fig. 9. Effect of time on the absorption of the Ag complex solution (Ag concentration of 20 ppm + 2 mL nano reagent solution with concentration of 1×10^{-4} M)

that after the time of 5 min, the absorbance of the prepared complex remains almost constant till time period of 24 h. The results of the study showed that the studied complex has a high stability and 5 min is the optimum time to complete

the reaction between silver ion (I) solution and the nano reagent solution.

Complex composition and stability constant

For the determination of the composition

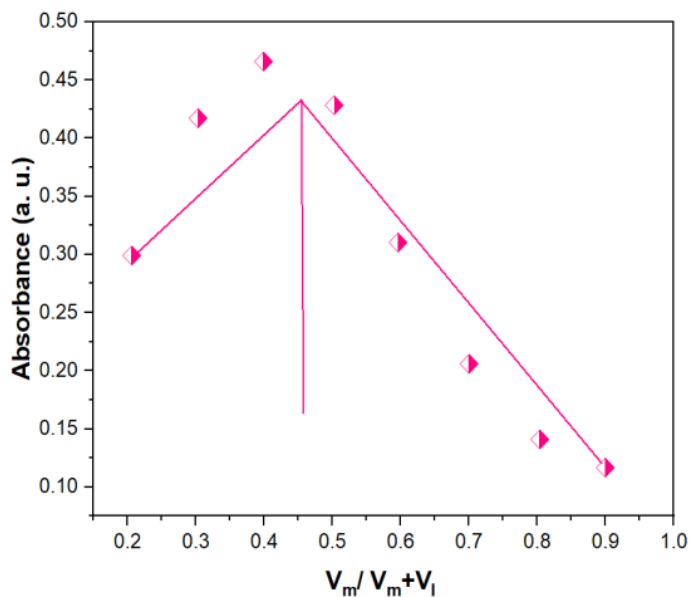


Fig. 10. Continuous variation method for Ag (I) complex with HMNTDABA at the pH value of 8.

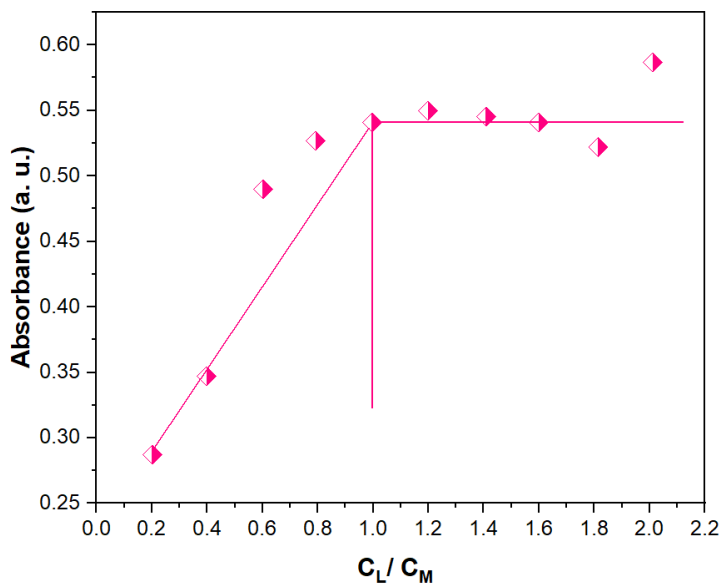


Fig. 11. Mole ratio method for Ag (I) complex with HMNTDABA at pH = 8.

and stability constant, both the continuous variation (Fig. 10) and the mole ratio approaches (Fig. 11) were used. It was observed that at pH = 8, the molar ratio of silver (I) ions to the nano organic reagent is 1:1 (metal: reagent) that was also confirmed by both approaches (continuous variation and the mole ratio). Following equation helps in determining the stability constant ($K_{st} = 0.5 \times 10^{-6}$) and the complex as follows:

$$K_{st} = \frac{1}{K_{ins}} \tag{1}$$

$$K_{ins} = \frac{(\alpha C)(n\alpha C)^2}{C(1-\alpha)} \cdot \alpha = \frac{A_m - A_s}{A_m} \tag{2}$$

where α represents degree of dissociation, c refers to the total concentration of the complex, n denotes mole ratio i.e., (1 to Ag(I)), A_m refers to the

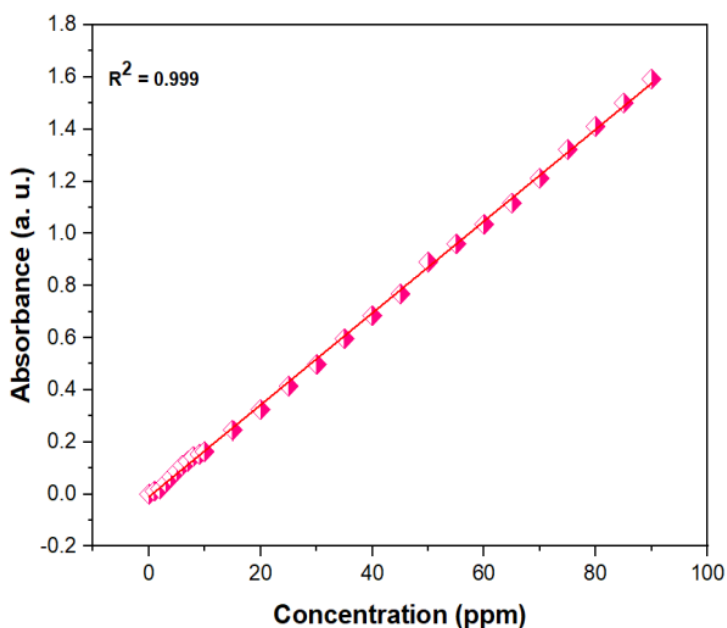


Fig. 12. Calibration curve of Ag (I) complex

Table 2. Analytical data for the proposed Ag (I) determination technique.

Analytical Parameter	Ag (I) /ppm
λ_{max}	563 nm
Regression equation	Y=0.0182x+0.3081
Molar absorptivity ($L \cdot mol^{-1} \cdot cm^{-1}$)	568.8×10^{-3}
Sandell Sensitivity	$0.001 L^{-1} \cdot gm \cdot cm$
Correlation coefficient (r)	0.9963
Detection limit(ppm)	0.085
Percent Relative error %	0.035%
Percent Recovery %	99.965
Composition of complex (M: L)	1:1
Linear dynamic range(ppm)	(1-80)
Standard deviation	0.001
Relative. Standard. Deviation %	0.14%

absorbance of a solution containing nano reagent two times higher than the silver amount and A_s refers to the absorbance of a solution containing a stoichiometric amounts of both [reagent] and [silver].

Characteristics of analysis

According to the experimental protocol, the calibration curve was made, and a good correlation coefficient was observed from the results (Fig. 12). The analytical parameters for this spectrophotometric analysis of Ag (I) with the synthesized nano reagent are summarized in Table 2.

Silver (I) complex investigation by interference

The divalent cations (Fe^{+2} , Ni^{+2} , Zn^{+2} , Pb^{+2} , Cu^{+2} , Cd^{+2}) formed complexes with the synthesized nano reagent, HMNTDABA, during its reaction with silver. The effects of these ions were examined and

the results are summarized in Table 3.

Determination of silver (I) in dental fillings

The procedure involved the dissolution of 0.1 g of dental filling in 10 mL of concentrated nitric acid. The resulting solution was filtered, and the filtrate was transferred to an opaque 100 mL volumetric flask, which was then diluted to the mark with distilled water for Ag measurement. Subsequently, half of the resulting solution was placed in a 50 mL volumetric flask, and the pH was adjusted to 8 using buffer solutions. Blocking agents were then added to inhibit the copper present in the solution. Finally, under optimal conditions, the silver ion (I) concentration was determined using the prepared nano reagent, HMNTDABA, via the spectroscopic method.

Followed by the application of the working method in a dental filling model (Australia by SDI Limited, Fig. 13), the proportions of its components



Fig. 13. Proportions of the components for the dental filling model.

Table 3. Effect of foreign ions in the determination of Ag(I) with concentration of 20ppm and suitable masking agent.

Foreign ion (40 ppm)	Error %	Masking agent (mL), [M]	Error % after adding masking agent
Fe^{+2}	0.018	Tartaric acid (1) [0.5]	0.002
Ni^{+2}	0.015	Tartaric acid (2.5), [0.5]	0.000
Zn^{+2}	0.023	$NaNO_2$ (1.5) [0.02]	0.003
Pb^{+2}	0.022	$NaNO_2$ (2), [0.02]	0.004
Cu^{+2}	0.016	Thiourea (1.5)[0.5]	0.003
Cd^{+2}	0.013	KI (0.5) [7.5×10^{-4}]	0.001

were determined including Ag = 40.0%, Cu = 28.7% and Sn = 31.3%. The results of the study revealed that the percentage of Ag ion was determined to be 39.44 % with the relative recovery of 98.6%. The results revealed that the studied method has good sensitivity and can be employed for the investigation of the Ag ions [53].

CONCLUSION

This study involved the synthesis of the novel nano azo reagent i.e., HMNTDABA for the preparation of the Ag (I)-complex. Successful synthesis of the nano reagent and its complex was investigated by the use of different characterization procedures including UV-Vis spectroscopy, infrared spectra, ¹H-NMR spectroscopy, XRD, FESEM and CHNS. Effect of pH, contact time, and temperature on complex formation was also investigated and results of the study revealed the pH of 8, time of 5 min and 25 °C as the optimum temperature. The applicability of the prepared silver complex was checked on a dental filling model to estimate the Ag ion using the spectroscopic method. The results revealed that the studied method has good sensitivity and can be used to estimate the silver ion.

CONFLICT OF INTEREST

The authors declare that there is no conflict of interests regarding the publication of this manuscript.

REFERENCES

1. Quang DT, Kim JS. Fluoro- and Chromogenic Chemodosimeters for Heavy Metal Ion Detection in Solution and Biospecimens. *Chem Rev.* 2010;110(10):6280-6301.
2. Spectrophotometric Determination of Hg (II) Using (E)-2-(4,5-bis(4-methoxyphenyl)-1H-imidazol-4-yl) diazenyl) benzoic acid as analytical reagent. *Journal of Pharmaceutical Negative Results.* 2022;13(S01).
3. S. Mohammed H. Synthesis, characterization, structure determination from powder X-ray diffraction data, and biological activity of azo dye of 3-aminopyridine and its complexes of Ni(II) and Cu(II). *Bull Chem Soc Ethiop.* 2021;34(3):523-532.
4. K. Jawad S, Sahib Mohammed Husien N. Solvent Extraction Method for Separation and Determination of Zn (II) by Using of Imidazole Derivative. *International Journal of Engineering and Technology.* 2018;7(4.36):553-556.
5. Spectrophotometric Determination of Metoclopramide- HCl in the standard raw and it compared with pharmaceuticals. *Journal of Pharmaceutical Negative Results.* 2021;21(2).
6. Atyaa Al, Radhy ND, Jasim LS. Synthesis and Characterization of Graphene Oxide/Hydrogel Composites and Their Applications to Adsorptive Removal Congo Red from Aqueous Solution. *Journal of Physics: Conference Series.* 2019;1234(1):012095.
7. Aljamali NM. Review in Azo Compounds and its Biological Activity. *Biochemistry and Analytical Biochemistry.* 2015;04(02).
8. Adnan S, Mohsen S, Jamel HO. Synthesis and Identification of novel azo-1,3,4-Thiadiazole Derivative and using to Spectrophotometric Determination for some of Transition metal Complexes. *Research Journal of Pharmacy and Technology.* 2018;11(7):2859.
9. Levin, David Saul, (born 28 Jan. 1962), Chief Executive, McGraw-Hill Education, New York, since 2014. *Who's Who: Oxford University Press;* 2007.
10. Mahmood Taher A, Ali Kadhim Kyhoiesh H, Shakir Waheeb A, Al-Adilee KJ, Jasim LS. Synthesis, characterization, biological activity, and modelling protein docking of divalent, trivalent, and tetravalent metal ion complexes of new azo dye ligand (N,N,O) derived from benzimidazole. *Results in Chemistry.* 2024;12:101911.
11. Hiroki A, Taguchi M. Development of Environmentally Friendly Cellulose Derivative-Based Hydrogels for Contact Lenses Using a Radiation Crosslinking Technique. *Applied Sciences.* 2021;11(19):9168.
12. Urry SA. *Fundamentals of Materials Science for Technologists: Properties, Testing and Laboratory Exercises*, L. Horath, Prentice Hall, Campus 400, Maylands Avenue, Hemel Hempstead, Herts HP2 7EZ. 1995. 550pp. Illustrated. £21.95. *The Aeronautical Journal.* 1996;100(996):255-255.
13. Haider R. Peripheral Vascular Disease. *Cardiology Research and Reports.* 2023;5(4):01-13.
14. Shah R. Spectrophotometric Micro determination of Silver(I) using Meloxicam as a New Analytical Reagent. *Oriental Journal of Chemistry.* 2016;32(1):499-507.
15. Stiles DA. I.C. Smith, B.L. Carson and F. Hoffmeister, Trace metals in the environment: volume 5— indium. *Anal Chim Acta.* 1980;113(1):200.
16. Books received. *Minerals and Energy - Raw Materials Report.* 1984;2(4):63-63.
17. Shahidi S, Wiener J. *Antibacterial Agents in Textile Industry. Antimicrobial Agents: InTech;* 2012.
18. Hadrup N, Lam HR. Oral toxicity of silver ions, silver nanoparticles and colloidal silver – A review. *Regulatory Toxicology and Pharmacology.* 2014;68(1):1-7.
19. Manzoori JL, Abdolmohammad-Zadeh H, Amjadi M. Ultra-trace determination of silver in water samples by electrothermal atomic absorption spectrometry after preconcentration with a ligand-less cloud point extraction methodology. *J Hazard Mater.* 2007;144(1-2):458-463.
20. Resano M, Aramendía M, García-Ruiz E, Crespo C, Belarra MA. Solid sampling-graphite furnace atomic absorption spectrometry for the direct determination of silver at trace and ultratrace levels. *Anal Chim Acta.* 2006;571(1):142-149.
21. Hu Q, Yang G, Zhao Y, Yin J. Determination of copper, nickel, cobalt, silver, lead, cadmium, and mercury ions in water by solid-phase extraction and the RP-HPLC with UV-Vis detection. *Analytical and Bioanalytical Chemistry.* 2003;375(6):831-835.
22. Moldovan Z. Spectrophotometric determination of nitrite by its catalytic effect on the oxidation of congo red with bromate. *Bull Chem Soc Ethiop.* 2012;26(2).
23. Eames JC, Matousek JP. Determination of silver in silicate rocks by furnace atomic absorption spectrometry. *Anal Chem.* 1980;52(8):1248-1251.
24. Kumar AP, Reddy PR, Reddy VK. Simultaneous second-derivative spectrophotometric determination of cobalt and vanadium using 2-hydroxy-3-methoxy benzaldehyde thiosemicarbazone. *J Anal Chem.* 2008;63(1):26-29.

25. Khomutova EG, Levkevich EA. Determination of the iridium micro-concentrations using a kinetic catalytic method. *Industrial laboratory Diagnostics of materials*. 2020;86(5):5-10.
26. Yuan C-G, Liang P, Zhang Y-Y. Determination of trace silver in environmental samples by room temperature ionic liquid-based preconcentration and flame atomic absorption spectrometry. *Microchimica Acta*. 2011;175(3-4):333-339.
27. Hill AA, Lipert RJ, Porter MD. Determination of colloidal and dissolved silver in water samples using colorimetric solid-phase extraction. *Talanta*. 2010;80(5):1606-1610.
28. Kabasakalis V. Fluorimetric Determination of Silver with Brilliant Green in Aqueous Systems and its Application in Photographic Fixing Solutions. *Anal Lett*. 1994;27(14):2789-2796.
29. Tseng K-H, Lee H-L, Tien D-C, Tang Y-L, Kao Y-S. A Study of Antibioactivity of Nanosilver Colloid and Silver Ion Solution. *Advances in Materials Science and Engineering*. 2014;2014:1-6.
30. Huang W, Liang Y, Deng Y, Cai Y, He Y. Prussian Blue nanoparticles as optical probes for visual and spectrophotometric determination of silver ions. *Microchimica Acta*. 2017;184(8):2959-2964.
31. Nagaraja P, Kumar MSH, Yathirajan HS. Silver-Enhanced Reduction of 2,3,5-Triphenyl-2H-tetrazolium by Semicarbazide for the Spectrophotometric Determination of Traces of Silver(I). *Anal Sci*. 2002;18(7):815-817.
32. Gao HW, Li YC, Zhang PF, Tao M, Wang L. Determination of Trace Amounts of Cadmium with p-Acetyl-Benzenediazoaminoozobenzene by Primary-Secondary Wavelength Spectrophotometry. *J Anal Chem*. 2001;56(11):1007-1010.
33. Errata for Guidelines for Cloud Seeding to Augment Precipitation, Third Edition, edited by Conrad G. Keyes, et al. *Guidelines for Cloud Seeding to Augment Precipitation: American Society of Civil Engineers*; 2016.
34. Guo XJ, Deng QL, Peng B, Gao JZ, Kang JW. Catalytic Spectrophotometry Determination of Ultratrace Amounts of Silver with Solubilizing Effect of Nonionic Surfactant. *Chin J Chem*. 2002;20(1):39-44.
35. Kassem MA. Development of a cloud-point extraction method for spectrophotometric nano determination of silver in real samples. *Analytical Methods*. 2015;7(16):6747-6754.
36. Batool M, Javed T, Wasim M, Zafar S, Din MI. Exploring the usability of Cedrus deodara sawdust for decontamination of wastewater containing crystal violet dye. *Desalination and Water Treatment*. 2021;224:433-448.
37. Shah A, Arjunan A, Thumma A, Zakharova J, Bolarinwa T, Devi S, et al. Adsorptive removal of arsenic from drinking water using KOH-modified sewage sludge-derived biochar. *Cleaner Water*. 2024;2:100022.
38. Shah A, Zakharova J, Batool M, Coley MP, Arjunan A, Hawkins AJ, et al. Removal of cadmium and zinc from water using sewage sludge-derived biochar. *Sustainable Chemistry for the Environment*. 2024;6:100118.
39. Mahde BW, Sultan AM, Mahdi MA, Jasim LS. Kinetic Adsorption and Release Study of Sulfadiazine Hydrochloride Drug from Aqueous Solutions on GO/P(AA-AM-MCC) Composite. *INTERNATIONAL JOURNAL OF Drug Delivery Technology*. 2022;12(04):1583-1589.
40. Mahdi MA, Oroumi G, Samimi F, Dawi EA, Abed MJ, Alzaidy AH, et al. Tailoring the innovative Lu2CrMnO6 double perovskite nanostructure as an efficient electrode materials for electrochemical hydrogen storage application. *Journal of Energy Storage*. 2024;88:111660.
41. Bukhari A, Javed T, Haider MN. Adsorptive exclusion of crystal violet dye from wastewater by using fish scales as an adsorbent. *J Dispersion Sci Technol*. 2022;44(11):2081-2092.
42. Imran MS, Javed T, Areej I, Haider MN. Sequestration of crystal violet dye from wastewater using low-cost coconut husk as a potential adsorbent. *Water Sci Technol*. 2022;85(8):2295-2317.
43. Urooj H, Javed T, Taj MB, Nouman Haider M. Adsorption of crystal violet dye from wastewater on Phyllanthus emblica fruit (PEF) powder: kinetic and thermodynamic. *Int J Environ Anal Chem*. 2023;104(19):7474-7499.
44. Mannan HA, Nadeem R, Bibi S, Javed T, Javed I, Nazir A, et al. Mesoporous activated TiO₂ /based biochar synthesized from fish scales as a proficient adsorbent for deracination of heavy metals from industrial efflux. *J Dispersion Sci Technol*. 2022;45(2):329-341.
45. Pourhoseini S, Enos RT, Murphy AE, Cai B, Lead JR. Characterization, bio-uptake and toxicity of polymer-coated silver nanoparticles and their interaction with human peripheral blood mononuclear cells. *Beilstein journal of nanotechnology*. 2021;12:282-294.
46. Barkur S, Lukose J, Chidangil S. Probing Nanoparticle-Cell Interaction Using Micro-Raman Spectroscopy: Silver and Gold Nanoparticle-Induced Stress Effects on Optically Trapped Live Red Blood Cells. *ACS omega*. 2020;5(3):1439-1447.
47. Sajeesh S, Sharma CP. Mucoadhesive hydrogel microparticles based on poly (methacrylic acid-vinyl pyrrolidone)-chitosan for oral drug delivery. *Drug Deliv*. 2010;18(4):227-235.
48. Kianipour S, Razavi FS, Hajizadeh-Oghaz M, Abdulsahib WK, Mahdi MA, Jasim LS, et al. The synthesis of the P/N-type NdCoO₃/g-C₃N₄ nano-heterojunction as a high-performance photocatalyst for the enhanced photocatalytic degradation of pollutants under visible-light irradiation. *Arabian Journal of Chemistry*. 2022;15(6):103840.
49. Gumus I, Karataş Y, Gülcan M. Silver nanoparticles stabilized by a metal-organic framework (MIL-101(Cr)) as an efficient catalyst for imine production from the dehydrogenative coupling of alcohols and amines. *Catalysis Science and Technology*. 2020;10(15):4990-4999.
50. Wei Y, Jiang H, Deng P. Direct quantification of cysteine and glutathione by ¹H NMR based on β-cyclodextrin modified silver nanoparticles. *Microchem J*. 2021;168:106471.
51. Hosseini M, Ghanbari M, Dawi EA, Mahdi MA, Ganduh SH, Jasim LS, et al. Investigations of nickel silicate for degradation of water-soluble organic pollutants. *Int J Hydrogen Energy*. 2024;61:307-315.
52. Kadhim Jawad S, Omran Kadhim M, Adnan Azooz E. Incorporation of Onium System with Cloud Point Extraction and Determination of Iron(III) and Mercury(II) in Different Samples. *Oriental Journal of Chemistry*. 2017;33(04):1879-1889.
53. Stencil R, Kasperski J, Pakieła W, Mertas A, Bobela E, Barszczewska-Rybarek I, et al. Properties of Experimental Dental Composites Containing Antibacterial Silver-Releasing Filler. *Materials* 2018, 11, 1031. *Materials (Basel, Switzerland)*. 2018;11(11):2173.